Heterogeneous & Homogeneous & Bio- & Nano-

CHEMCATCHEM

CATALYSIS

Accepted Article

Title: Facile synthesis of Cu@CeO₂ and its catalytic behavior for hydrogenation of methyl acetate to ethanol

Authors: Yue Wang, Yujun Zhao, Jing Lv, and Xinbin Ma

To be cited as: *ChemCatChem* 10.1002/cctc.201700111

Link to VoR: http://dx.doi.org/10.1002/cctc.201700111

A Journal of ChemPubSoc Europe

WILEY-VCH

www.chemcatchem.org

Facile synthesis of Cu@CeO₂ and its catalytic behavior for hydrogenation of methyl acetate to ethanol

Yue Wang, Yujun Zhao, Jing Lv, Xinbin Ma*[a]

Abstract: Hydrogenation of methyl acetate (MA) is one of the key steps in ethanol synthesis from syngas. Given the previous study, synergy of Cu^0 and Cu^+ species is the crux to improve the catalytic performance. However, neither of Cu^0 and Cu^+ is easily to maintain in the reaction conditions of abundant H_2 and high temperature. Here, a Cu@CeO_2 core-shell catalyst was fabricated by using facile sol-gel method and exhibited excellent activity and stability in MA hydrogenation. It is revealed that the Cu@CeO_2 core-shell structure can not only prevent the metallic copper particles from migration and aggregation, but also significantly increase the amount of Cu^+ species by enlarging the intimate contact areas of copper and ceria. Furthermore, the Cu^0 and Cu^+ species are well-distributed on the interface between the Cu core and CeO_2 shell. The close relative position of the two active sites is probably the main reason for the enhanced synergetic effect in hydrogenation of MA. These new insights of the core-shell structure-function relationship introduce new possibilities for the rational design of catalysts.

Ethanol, as a versatile feedstock for chemical synthesis and a promising fuel alternative or additive, has presented great commercial potential in the market.[1] Recently, a new route of ethanol synthesis from syngas via dimethyl ether carbonylation and methyl acetate (MA) hydrogenation was proposed (Scheme S1 in Supporting Information), which shows an attractive prospect in industry due to its high atomic economy and environmental friendliness.[2] Hydrogenation of MA as one of the key steps has drawn lots of attentions from both the industry and academy.

Considering the excellent selective activity on C-O/C=O bonds hydrogenolysis, Cu-based catalysts have been widely used in vapor-phase hydrogenation of esters (such as MA[3], dimethyl oxalate[4] and furfural[5]). With development on understanding of the catalytic essence, it has been demonstrated that synergy of Cu^0 and Cu^+ species could remarkably enhance the catalytic performance for ester hydrogenations, where Cu^0 facilitates the H_2 decomposition and Cu^+ adsorbs and activates the methoxy or acyl species.[3b, 6] However, in the reaction conditions of abundant H_2 atmosphere (the molar ratio of H_2/MA is 80 in feed) and high temperature (usually above 200 ºC), Cu^0 nanoparticles tend to migrate and aggregate, and Cu^+ species are prone to be reduced. Thus, it becomes essential to design and fabricate catalysts with stable coexisting and highly dispersed Cu^0 and Cu^+ species for MA hydrogenation.

In the published literatures, it has been proposed that introducing some metal oxides with oxygen vacancies (such as CeO_2[7], ZrO_2[8], TiO_2[9], LaO_x[10], MnO_x[11]) as supports or additives into Cu-based catalysts could increase the metallic copper dispersion and enrich the surface Cu^+ sites. The strong interaction between the oxides and Cu species located at interfacial sites is presumably responsible for the improvement of catalytic activity and stability in ester hydrogenations.[7-11] However, the area of interface is very limited in conventional supported catalysts, where the metal particles are set on a bulk matrix of substrate oxides (like Scheme 1a). Thus, if frame structure of the catalyst is composed of metal particles confined with the support oxides particles, it would not only improve the sintering resistance, but also enlarge the interfacial area, expectedly leading to enhanced performance of the catalyst in hydrogenation process.

Here, we introduced a sol-gel method for facile and efficient synthesis of Cu@CeO_2 core-shell catalysts, which displayed remarkable efficiency and stability towards MA hydrogenation. CeO_2 was chosen as the support because the metal/ceria-based system is well-known to exhibit strong metal-support interaction effects.[12] Due to the high oxygen storage and release capacity, excellent redox property, and facile oxygen vacancy formation of CeO_2, it has been proved that Cu^+ species exist in the reduced Cu/CeO_2 catalysts[7], which can meets the demands of catalyst for MA hydrogenation. To further investigate the structure-function relationship of the core-shell structured catalyst, a Cu/CeO_2-IM catalyst was prepared as the contrastive sample by using conventional impregnation method. And for reasonable comparison, its support was synthesized through the same process as Cu@CeO_2 to exclude the effects of the particle size and oxygen vacancy on the catalytic performance.

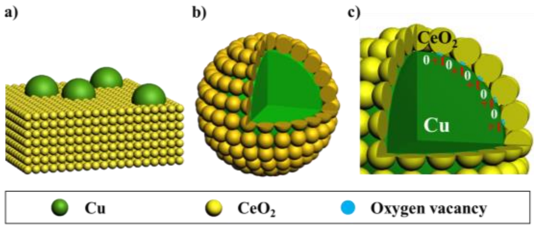

Scheme 1. Schematic illustration of a) Cu/CeO_2-IM prepared by conventional impregnation method, b) Cu@CeO_2 fabricated by the facile sol-gel method, c) Cu^0 and Cu^+ distribution of the reduced Cu@CeO_2 catalyst.

Cu@CeO_2 and Cu/CeO_2-IM with 30 wt.% copper loading were prepared as mentioned respectively and their transmission electron microscopy (TEM) images are displayed in Figure 1.

---

[a] Dr. Y. Wang, Dr. Y. Zhao, Dr. J. Lv, Prof, X. Ma
Key Laboratory for Green Chemical Technology of Ministry of Education, Collaborative Innovation Centre of Chemical Science and Engineering, School of Chemical Engineering and Technology
Tianjin University
Tianjin, 300072 (P.R. China)
E-mail: xbma@tju.edu.cn

Supporting information for this article is given via a link at the end of the document.

10.1002/cctc.201700111

After reduced at 300 °C for 4h, the 30Cu@CeO_2 catalyst displays a desired core-shell structure, in which the copper particles are confined by many surrounding CeO_2 nanoparticles. Applying the electron energy loss spectroscopy (EELS) spectrum imaging for further confirmation, the Cu cores are clearly separated and embraced by uniformly dispersed Ce and O elements (Figure 1). Notably, the size of metallic copper particles in 30Cu@CeO_2 is only about 16 nm, while that in 30Cu/CeO_2-IM becomes above 50 nm after reduction. Meanwhile, according to their x-ray diffraction (XRD) patterns (Figure 2), consistent results are obtained. The peaks at 2θ angles of 43.3°, 50.4° and 74.1° attributed to metallic Cu species (JCPDS 04-0836) are more weaken and broader in the reduced 30Cu@CeO_2 sample than those in the 30Cu/CeO_2-IM, indicating that a much smaller size of metallic copper particles in 30Cu@CeO_2 (Table 1). Thus, it can be conclude that the core-shell structure has a great impact on preventing the migration and aggregation of the metallic copper particles.

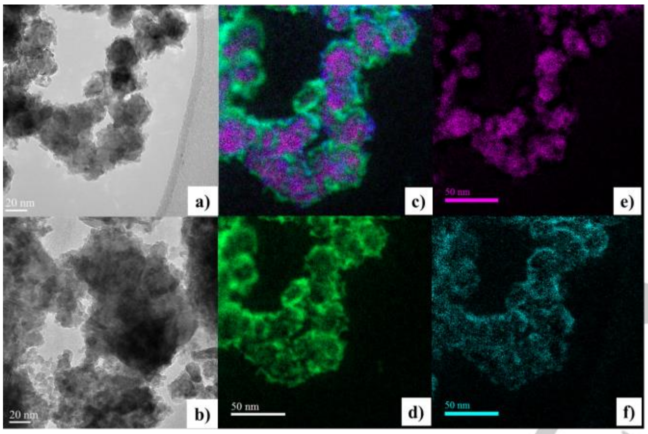

Figure 1. TEM images of the reduced a) 30Cu@CeO_2 and b) 30Cu/CeO_2-IM; the corresponding EELS spectrum imaging of the reduced 30Cu@CeO_2: c) the composite image, d) the Ce-M edge map, e) the Cu-L edge map and f) the O-K edge map.

As metioned before, the support of 30Cu/CeO_2-IM was prepared by the same sol-gel method for comparision. It can be seen that both of the supprot and shell structure are composed of 3-5 nm small CeO_2 nanoparticles (Figure 1). Moreover, in the XRD patterns (Figure 2), the peaks marked with triangles can be indexed to the cubic fluorite CeO_2 (JCPDF04-0593), which are similar in both of the samples. And the broad shape of peaks implies the small size of ceira particles, agreed with the TEM results. The resemblance of CeO_2 supports allows us to reveal the effect of strucures on copper species distribution.

For further understanding the roles of core-shell structure in catalysis, the amounts of surface active sites were qualitatively and quantitatively characterized by using the N_2O-CO titration[11, 13], x-ray photoelectron spectroscopy (XPS) and Auger electron spectroscopy (AES) (Detailed precudures are described in the Supporting Information). As shown in Figure 3a, there are no Cu_{2p} satellite peaks observed at binding energy of 942-944 eV, which demostrates all the copper species had been reduced to Cu^0 or Cu^+ after reduction.[14] In this case, the overlapping peaks at 567.4 and 570.0 eV in the Cu LMM AES spectra can be ascribed to Cu^0 and Cu^+ species respectively, of which the integral areas were employed to calculate the molar ratios of surface $Cu^+/(Cu^0+Cu^+)$, denoted as $X_{Cu(I)}$ (Table 1).[14] Notably, the higher binding energy for Cu^+ (Figure 3b) than the bulk value indicates that there is an strong interaction between Cu^+ and CeO_x species.[14] The propotion of surface Cu^+ species in 30Cu@CeO_2 is as large as 71.0%, while it is only 13.4% in the 30Cu/CeO_2-IM. Combined with the N_2O-CO titration results, the surface areas of copper species were obtained (listed in Table 1). Because of the aggregated metallic Cu particles, the Cu^0 surface area ($S_{Cu(0)}$) in 30Cu/CeO_2-IM is much smaller than that of 30Cu@CeO_2. However, the reason for the difference on Cu^+ surface areas ($S_{Cu(I)}$) and $X_{Cu(I)}$ of the two catalysts needs a further discussion.

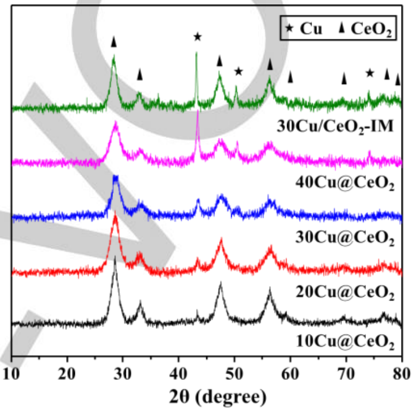

Figure 2. XRD patterns of the reduced Cu@CeO_2 and 30Cu/CeO_2-IM catalysts.

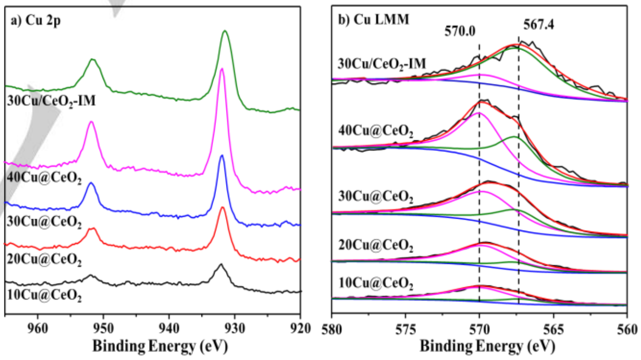

Figure 3. a) Cu 2p XPS spectra; b) Cu LMM AES spectra of the reduced Cu@CeO_2 and 30Cu/CeO_2-IM catalysts.

According to the literatures, the mobile oxygens can be released from the lattice of CeO_2 and form lots of surface oxygen vacancies during reduction.[12, 15] As a result, the Cu^+ species could be generated and stabilized by the interaction between Cu particles and the oxygen vacancies of CeO_2 support.[11, 16] Notably, no peak ascribed to Cu_2O species appears in the XRD patterns, which implies the highly dispersed Cu^+ species are formed by the strong interaction of Cu-CeO_x species as well. Given the similar properties of CeO_2 supports, their ability of developing Cu^+ species can be considered as a constant. Thus, the intimate contact area between the Cu and CeO_x species becomes the key factor influencing the $X_{Cu(I)}$. As shown in Scheme 1, in the 30Cu/CeO_2-IM catalyst, only the bottom area of Cu particles can contact with the CeO_2 support, while the whole surface of Cu particles are covered by CeO_2 nanoparticles in the 30Cu@CeO_2.

10.1002/cctc.201700111

Thus, it can be deduced that the core-shell structure could significantly increased the interfacial area between Cu and CeO_2 nanoparticles, leading to an great enrichment of Cu^+ species, which were generated and stablized by the strong interaction of Cu-CeO_x species.

The vapor-phase hydrogenation of MA was carried out here to study the catalytic activity and stability of the reduced 30Cu/CeO_2-IM and 30Cu@CeO_2 catalysts. The reaction was carried out at 215 ºC, 2.5 MPa, 80 molar ratio of H_2/MA in feed. As shown in Figure 4, the 30Cu@CeO_2 exhibited a much higher activity and stability in comparison with the 30Cu/CeO_2-IM catalyst. It achieved both of the MA conversion and the selectivity of ethanol approximately 100% at a weight-based liquid hourly space velocity (WLHSV) of 1.0 h^{-1}. Furthermore, there is no obvious change in the catalytic performance of 30Cu@CeO_2 for 160 hours, while the MA conversion of 30Cu/CeO_2-IM decreased rapidly in 10 hours. Thus, the core-shell structured 30Cu@CeO_2 displayed a remarkably improved catalytic activity and stability in MA hydrogenation, which is probably attributed to the high dispersion of Cu^0 particles and the enrichment of surface Cu^+ species.[10]

Table 1. Physicochemical properties of the reduced Cu@CeO_2 and 30Cu/CeO_2-IM catalysts.

Catalysts	d_{Cu}[a] (nm)	D_{Cu}[b] (nm)	$X_{Cu(I)}$[c] (%)	$S_{Cu(0)}$[d] (m^2/g)	$S_{Cu(I)}$[d] (m^2/g)	SX_{Cu}[e] (m^2/g)
30Cu/CeO_2-IM	56.3	N.A.[f]	13.4	0.9	0.1	3.6
10Cu@CeO_2	9.2	8.8	88.2	2.1	15.5	7.3
20Cu@CeO_2	14.5	14.3	83.1	2.6	13.0	9.2
30Cu@CeO_2	16.0	15.7	71.0	3.9	9.5	12.4
40Cu@CeO_2	30.4	N.A.	56.5	4.6	6.0	11.6

[a] Average diameter of Cu particles calculated from XRD patterns by using Scherrer equation. [b] Average diameter of Cu particles measured from the TEM images. [c] Cu^+/(Cu^0+Cu^+) obtained from Cu LMM AES spectra. [d] Surface area of Cu^0 or Cu^+ species calculated from the results of N_2O-CO titration and $X_{Cu(I)}$, assuming that Cu^0 and Cu^+ occupy identical atomic areas and have identical atomic sensitivity factors. [e] Surface area of Cu core particles based on d_{Cu}. [f] Not available because the Cu particles in 30Cu/CeO_2-IM and 40Cu@CeO_2 are too irregular-shaped and wide-distributed to measure.

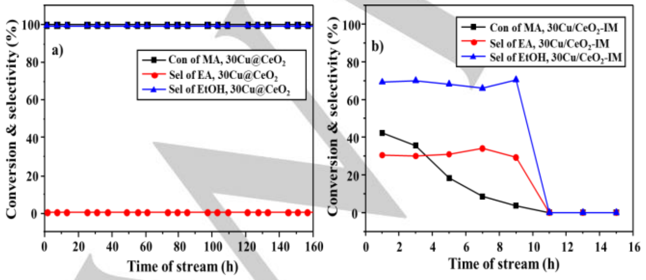

Figure 4. Catalytic activity and stability of the reduced a) 30Cu@CeO_2 and b) 30Cu/CeO_2-IM catalysts for MA hydrogenation. Reaction conditions: 0.5 g catalyst, 215 ºC, 2.5 MPa, H_2/MA = 80, WLHSV = 1.0 h^{-1}.

In order to explore the composition range of applying the sol-gel method in catalysts fabrication, Cu@CeO_2 catalysts with varied Cu loadings (10-40 wt.%) were prepared and characterized. As shown in Figure S1 in the Supporting Information, the core-shell structures are successfully formed in all the catalysts. However, as the copper contents increased, the size of metallic Cu particles grew up and the CeO_2 shell became thinner and thinner. It is noteworthy that when the copper loading is up to 40 wt.%, the size of metallic Cu particles greatly increases to about 30 nm, while it displays no obvious change in 20Cu@CeO_2 and 30Cu@CeO_2 catalysts. Furthermore, the size of metallic Cu particles in 40Cu@CeO_2 also becomes wide-distributed and scattered, while it exhibits a relative narrow distribution in the other catalysts. Meanwhile, the peak at 2θ of 43.3º in the reduced 40Cu@CeO_2 is significant narrow-shaped and much stronger than the other ones (Figure 2), indicating the large size of Cu^0 particles as well. The calculated size of metallic copper particles by using Scherrer equation is consistent with the TEM results (Table 1). The rapidly growth of Cu^0 particles in 40Cu@CeO_2 is probably because the reduced proportion of CeO_2 is not enough to cover the copper species during reduction, which is consist with the analysis results of pore properties (Table S1 and Figure S2 in the Supporting Information). It can be supported by the decreased $X_{Cu(I)}$ as well (Figure 3 and Table 1), which reflects the reduction of contact areas between Cu and CeO_2 nanoparticles.

Combined with N_2O-CO titration results, the surface areas of copper species of Cu@CeO_2 catalysts were obtained (Table 1). With the increase of copper contents, the $S_{Cu(I)}$ decreases while the $S_{Cu(0)}$ increases. It is demonstrated that even though the Cu^0 particles grow up, the surface areas of active sites still dominantly affected by the composition of catalysts. Additionally, the proportions of Cu^+ species obtained in the Cu@CeO_2 catalysts are much higher than the reported Cu-based catalysts for ester hydrogenation.[4a, 6, 10, 17] Besides the effect of core-shell structure, the extremely small size of CeO_2 supports probably plays an important role in fabricating catalysts with such a high $X_{Cu(I)}$ as well. The small sized particles is in favor of enlarging the available surface areas for intimate contact with the core, as well as enhancing the metal-support interaction.[18]

For investigating how the synergetic effect of Cu^0 and Cu^+ species works in the MA hydrogenation, the catalytic activity tests of Cu@CeO_2 were carried out (details shown in Figure S3 of the Supporting Information). 30Cu@CeO_2 displayed the best activity in MA conversion and selectivity of ethanol. Furthermore, assuming the Cu^+ ions occupies the same area as that of the Cu^0 atoms, the turnover frequency values ($TOF_{Cu(0)}$ and $TOF_{Cu(I)}$) were calculated (Figure 5) on the basis of the surface areas of Cu^0 and Cu^+ species respectively, combined with the corresponding copper contents (measured by ICP-OES and listed in Table S1 of Supporting Information).[3b] The $TOF_{Cu(I)}$ linearly increases with the increasing amounts of surface Cu^0 species, whereas $TOF_{Cu(0)}$ displays independent changes with the surface area of Cu^+ species. This phenomenon is consistent with our previous work[3b], which demonstrates only if the metallic copper surface area is above a certain value (20 m^2/g in the Cu/SiO_2 catalysts), the effect of Cu^+ on catalysis would emerge, whereas the catalytic performance is primarily influenced by the Cu^0 species.

Interestingly, both of the $TOF_{Cu(I)}$ and $TOF_{Cu(0)}$ of the Cu@CeO_2 catalysts are much higher than the reported ones[3b, 4a, 10, 19], indicating a more efficient utilization of the active sites in catalysis. It may be resulted from the enhanced synergetic effect of Cu^0 and

Cu^+ species by the unique core-shell structure of $Cu@CeO_2$ catalysts. We found out that the surface area of Cu cores, i.e. the interface area between Cu and CeO_2 species (SX_{Cu}), demonstrates a positive correlation with the total surface areas of Cu^0 and Cu^+ species (Table 1), indicating a uniform distribution of the two active sites on the interface between Cu core and CeO_2 shell. Thus, according to the Cu^+ species formed by the Cu-CeO_x species, both of the Cu^0 and Cu^+ would generate on the interface between the Cu core and CeO_2 shell. This distribution manner (Scheme 1c) can achieve a close relative position of the two active sites, which would effectively enhance the synergetic effect on the catalysis for MA hydrogenation.

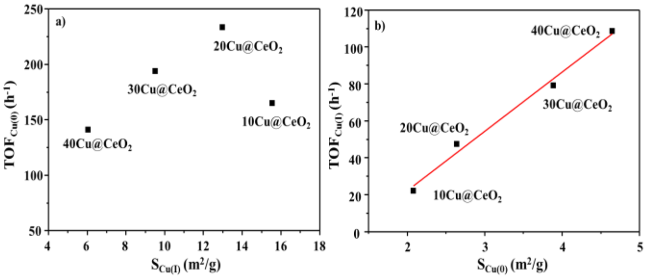

Figure 5. Effects of a) Cu^+ active sites and b) Cu^0 active sites of $Cu@CeO_2$ catalysts on the catalytic performance for MA hydrogenation, respectively.

In summary, we introduced a sol-gel method for fabricating the $Cu@CeO_2$ catalysts for ethanol production via MA hydrogenation, where the Cu core is surrounded by the shell composed of many small CeO_2 nanoparticles. It is demonstrated the core-shell structure can effectively prevent the metallic copper species from migration and aggregation, which greatly enhanced the stability of catalyst. At the same time, the core-shell structure would enlarge the contact areas of Cu and CeO_2 particles and enrich the surface Cu^+ concentration, owing to the strong interaction of Cu-CeO_x species, which significantly improved the catalytic activity for MA hydrogenation. Moreover, the Cu^0 and Cu^+ species are well-distributed on the interface between the Cu core and CeO_2 shell, leading to a close relative position of these two active sites and an enhanced synergetic catalysis effect. Owing to its facile procedures and efficient productivity, the sol-gel method displays great potential in industry for core-shell structured metal-oxides material synthesis. And the insights to the core-shell structure-functional relationship introduce new possibilities for the rational design of catalysts.

Experimental Section

The $Cu@CeO_2$ catalyst was fabricated by a facile and efficient sol-gel method. Briefly, copper nitrate and cerium nitrate with calculated proportions were dissolved with 25 mL deionized water. Meanwhile, dissolve a certain amount of citric acid (the mole ratio of citric acid / (copper nitrate + cerium nitrate) is 1:1) into another 25 mL deionized water. These two solutions were blended together and kept stirring for 1 h at room temperature. Then, the mixture was heated to 65 °C for 1 h under vacuum to remove extra water and formed a gelatinous substance. After dried at 100 °C for 10 h, the sample was calcined in static air at 300°C for 2 h to decompose the citric acid and then heated to 400 °C for 2 h. The temperature ramp for calcination was 1 °C/min. Then the resulting solid was tabled, crushed and sieved to 40-60 mesh for reaction. Additionally, the contrastive Cu/CeO_2-IM sample was prepared by a typical incipient-wetness impregnation method. The support CeO_2 nanoparticles were synthesized through procedures as the same as above without the addition of copper nitrate, but only calcined at 300°C for 2 h. After impregnation, the obtained solid was calcined again at 400 °C for 2 h.

The materials information, detailed procedures of characterizations (such as TEM, XRD, XPS, and N_2O-CO titration), catalytic activity evaluation and products analysis were described in the Supporting Information.

Acknowledgements

This research was supported by the National Natural Science Foundation of China (21325626, 91434127) and the Program of Introducing Talents of Discipline to Universities (B06006).

Keywords: Copper-based catalyst • core-shell structure • ethanol • heterogeneous catalysis • hydrogenation

[1] J. Goldemberg, *Science* **2007**, *315*, 808-810.
[2] a) X. San, Y. Zhang, W. Shen, N. Tsubaki, *Energy & Fuels* **2009**, *23*, 2843-2844; b) X. Li, X. San, Y. Zhang, T. Ichii, M. Meng, Y. Tan, N. Tsubaki, *Chemsuschem* **2010**, *3*, 1192-1199.
[3] Y. Wang, Y. Shen, Y. Zhao, J. Lv, S. Wang, X. Ma, *ACS Catal.* **2015**, *5*, 6200-6208.
[4] a) J. Gong, H. Yue, Y. Zhao, S. Zhao, L. Zhao, J. Lv, S. Wang, X. Ma, *J. Am. Chem. Soc.* **2012**, *134*, 13922-13925; b) H. Yue, Y. Zhao, S. Zhao, B. Wang, X. Ma, J. Gong, *Nature Commun.* **2013**, *4*, 2339.
[5] S. Sitthisa, T. Sooknoi, Y. Ma, P. B. Balbuena, D. E. Resasco, *J. Catal.* **2011**, *277*, 1-13.
[6] A. Yin, X. Guo, W. Dai, K. Fan, *J. Phys. Chem. C* **2009**, *113*, 11003-11013.
[7] C. Ye, C. Guo, J. Zhang, *Fuel Process. Technol.* **2016**, *143*, 219-224.
[8] Y. Zhu, X. Kong, S. Zhu, F. Dong, H. Zheng, Y. Zhu, Y. Li, *Appl. Catal. B-Environ.* **2015**, *166–167*, 551-559.
[9] C. Wen, A. Yin, Y. Cui, X. Yang, W.-L. Dai, K. Fan, *Appl.Catal. A-Gen.* **2013**, *458*, 82-89.
[10] X. Zheng, H. Lin, J. Zheng, X. Duan, Y. Yuan, *ACS Catal.* **2013**, *3*, 2738-2749.
[11] Q. Hu, L. Yang, G. Fan, F. Li, *J. Catal.* **2016**, *340*, 184-195.
[12] C. Sun, H. Li, L. Chen, *Energ. Environ. Sci.* **2012**, *5*, 8475-8505.
[13] M. B. Fichtl, J. Schumann, I. Kasatkin, N. Jacobsen, M. Behrens, R. Schlögl, M. Muhler, O. Hinrichsen, *Angew. Chem. Int. Ed.* **2014**, *53*, 7043-7047.
[14] L. Chen, P. Guo, M. Qiao, S. Yan, H. Li, W. Shen, H. Xu, K. Fan, *J. Catal.* **2008**, *257*, 172-180.
[15] M. Ganduglia-Pirovano, A. Hofmann, J. Sauer, *Sur. Sci. Rep.* **2007**, *62*, 219-270.
[16] Y. Liu, K. Murata, M. Inaba, I. Takahara, *Fuel Process. Technol.* **2013**, *110*, 206-213.
[17] C. L. Ye, C. L. Guo, J. L. Zhang, *Fuel Process. Technol.* **2016**, *143*, 219-224.
[18] S. Li, C. Zhang, Z. Huang, G. Wu, J. Gong, *Chem. Commun.* **2013**, *49*, 4226-4228.
[19] D. Wang, G. Yang, Q. Ma, M. Wu, Y. Tan, Y. Yoneyama, N. Tsubaki, *ACS Catal.* **2012**, *2*, 1958-1966.

Table of Contents

COMMUNICATION

New insights of core-shell structure-function relationship

The core-shell structure of Cu@CeO$_2$ not only prevented the aggregation of Cu particles, but also enlarged the contact area between Cu and CeO$_2$, which greatly increased the Cu$^+$ surface area. Moreover, Cu^0 and Cu$^+$ active sites were well-distributed on the core-shell interface, resulting in a close relative position and an enhanced synergetic catalysis effect for methyl acetate hydrogenztion.

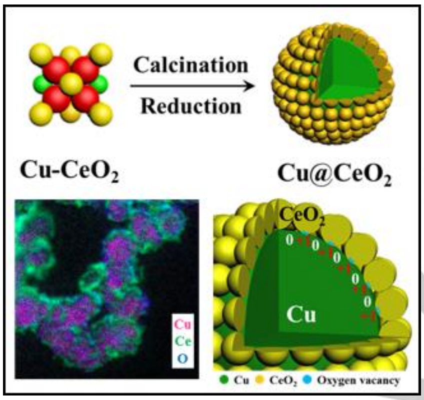

*Yue Wang, Yujun Zhao, Jing Lv, Xinbin Ma**

Page No. – Page No.

Facile synthesis of Cu@CeO$_2$ and its catalytic behavior for hydrogenation of methyl acetate to ethanol